



ChemComm

**Modelling 'Histidine Brace' Motif in Mononuclear Copper  
Monooxygenases**

Journal:	<i>ChemComm</i>
Manuscript ID	CC-COM-02-2020-001392.R2
Article Type:	Communication

SCHOLARONE™  
Manuscripts

## COMMUNICATION

## Modelling 'Histidine Brace' Motif in Mononuclear Copper Monoxygenases

Arisa Fukatsu,<sup>a</sup> Yuma Morimoto,<sup>a</sup> Hideki Sugimoto<sup>a</sup> and Shinobu Itoh<sup>\*a</sup>

Received 00th January 20xx,  
Accepted 00th January 20xx

DOI: 10.1039/x0xx00000x

A mononuclear copper complex bearing 'Histidine Brace' is synthesised and characterised as an active-site model of mononuclear copper monoxygenases such as lytic polysaccharide monoxygenases (LPMOs) and particulate methane monoxygenase (pMMO). The complex has similar structural and functional features to those of the active sites of the enzymes.

Understanding the mechanisms of monoxygenase reactions in biological systems is highly important as a guide to develop a cost-effective process for the production of liquid fuels from primary energy sources such as biomass and natural gas.<sup>1-3</sup> Lytic polysaccharide monoxygenases (LPMOs) catalyses the oxidative degradation of polysaccharides such as cellulose and chitin,<sup>4-6</sup> being expected as biomass sources. Various types of LPMOs have already been identified, and their geometrical properties and physical properties are under intense investigations.<sup>7, 8</sup> A characteristic structural unit found in the active sites of LPMOs consists of an amino group and a side chain of the *N*-terminal histidine with a side chain of a second histidine to create a T-shaped N<sub>3</sub> geometry at the copper reaction centre, so-called Histidine Brace (Figs. 1a and 1b).<sup>5</sup> A notable feature of the Histidine Brace is the twist angle between the two histidine imidazole rings situated at the *trans*-position is around 70°. Such a large twist angle is significantly different from the twist angles in many analogous copper(II) complexes bearing two heterocycle donor groups at the *trans*-position, that is usually less than 30°.<sup>7</sup>

Meanwhile, particulate methane monoxygenase (pMMO) is known as one of the rare enzymes that catalyse the selective production of methanol from methane, which is the main component of natural gas.<sup>9-11</sup> Although, the structure of the active site of pMMO has been highly controversial,<sup>9, 12-14</sup> the

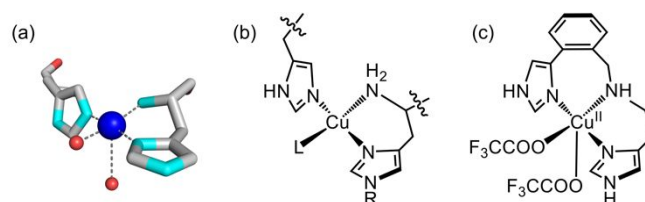


Fig. 1. (a) Crystal structure of the active site of LPMO (PDB: 5FJQ). Schematic structures of (b) Histidine Brace and (c) Cu<sup>II</sup>(LH<sub>3</sub>)(tfa)<sub>2</sub>.

recent studies have suggested the existence of a mononuclear copper active site with a Histidine Brace like coordination environment.<sup>15-17</sup>

It is remarkable that Histidine Brace is found as a common structural motif of the active sites of LPMOs and pMMO, which catalyses oxidation of the inert C–H bond of polysaccharides and methane (bond dissociation energy is around or higher than 100 kcal/mol). Therefore, this characteristic structural motif should be worth considering in the design of ligands to emulate the enzyme active sites. To mimic the structural motif of Histidine Brace, we designed a new ligand with the concepts as follows. The ligand should be a tridentate ligand bearing two imidazole groups at the *trans*-positions together with an alkylamine group to create a T-shaped N<sub>3</sub> geometry for the bound copper ion. A large twist angle between the two imidazole groups should be maintained as in the enzyme active sites of LPMOs. Furthermore, the ligand should involve imidazole group(s) having an acidic N–H proton(s) as the natural enzymes do.

<sup>a</sup> Department of Material and Life Science, Division of Advanced Science and Biotechnology, Graduate School of Engineering, Osaka University, 2-1 Yamadaoka, Suita, Osaka 565-0871, Japan. E-mail: shinobu@mls.eng.osaka-u.ac.jp

† Electronic Supplementary Information (ESI) available: Experimental details, results of spectroscopic measurements, electrochemical measurements and catalytic reactions. CCDC 1985635. See DOI: 10.1039/x0xx00000x

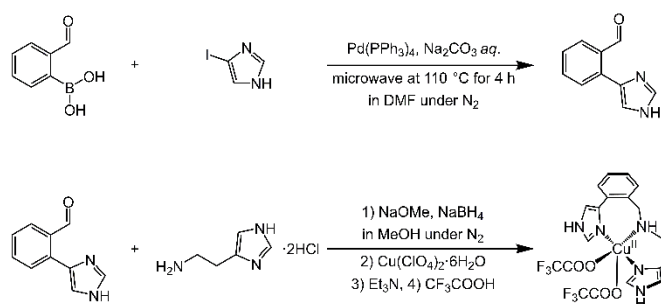
Recently, synthetic bioinorganic chemists have been trying to develop active-site model complexes for the mononuclear copper monooxygenases.<sup>18–21</sup> In those cases, however, pyridine, *N*-methylimidazole or *N*-methylbenzimidazole was used instead of imidazole having a dissociative N-H proton. In the cases of the *N*-methylimidazole and *N*-methylbenzimidazole containing ligands, the five-membered heterocyclic donor group are connected to the alkyl tether group at the 2-position (the position between the two nitrogen atoms), which is different from the substituent position of histidine (at 4-position) in nature. Moreover, the twist angles of the two heterocyclic donor groups situated at the *trans*-positions in those model complexes are much smaller (less than 30°) than that of the Histidine Brace in the biological system.

Based on these backgrounds, we herein designed and synthesised a new supporting ligand **LH<sub>3</sub>** (*N*-(2-(1*H*-imidazol-4-yl)-benzyl)histamine) and its copper(II) complex **Cu<sup>II</sup>(LH<sub>3</sub>)(tfa)<sub>2</sub>** (tfa = trifluoroacetate) (Fig. 1c) to provide more precise model complex of the active sites of copper monooxygenases. A phenyl group was introduced as a connector between the amine nitrogen atom of histamine and the imidazolyl group at its 4-position. This novel tridentate ligand **LH<sub>3</sub>** meets the structural requirements of the Histidine Brace, including the large twist angle of the two imidazolyl groups at the *trans*-position.

**Cu<sup>II</sup>(LH<sub>3</sub>)(tfa)<sub>2</sub>** was prepared according to Scheme 1. The ligand precursor, 2-(1*H*-imidazol-4-yl)-benzaldehyde, was synthesised by Suzuki-Miyaura coupling between 4-iodo-1*H*-imidazole and 2-formylphenyl boronic acid in the presence of Pd(PPh<sub>3</sub>)<sub>4</sub> in *N,N*-dimethylformamide (DMF) under inert conditions with a little modification of the previously reported procedure.<sup>22</sup> Then, the reductive amination of the benzaldehyde derivative with histamine provided the ligand **LH<sub>3</sub>**.<sup>23</sup> Since **LH<sub>3</sub>** was not stable enough for purification by silica gel chromatography or crystallisation, it was used for complexation with Cu(ClO<sub>4</sub>)<sub>2</sub> without isolation. Addition of Cu(ClO<sub>4</sub>)<sub>2</sub> to the solution of **LH<sub>3</sub>** caused a colour change from brown to blue, from which blue powder gradually precipitated. The resulting blue powder was insoluble in ordinary solvents. Treatment of the complex with trifluoroacetic acid was found to solubilise the complex, and the complex was recrystallised from methanol and diethyl ether to give blue crystals of **Cu<sup>II</sup>(LH<sub>3</sub>)(tfa)<sub>2</sub>**. In a neutral or basic conditions, the imidazolyl N-H group was probably deprotonated and coordinated to the copper(II) ion of the neighbouring copper(II) complex to make an insoluble polymeric structure. The results of ESI-TOF-MS and elemental analysis were matched well expected ones as the copper(II) complex (See the Supplementary Information).

The crystal structure of **Cu<sup>II</sup>(LH<sub>3</sub>)(tfa)<sub>2</sub>** is shown in Fig. 2, and the crystallographic data is summarised in Table S1. The copper centre exhibits a square pyramidal geometry with  $\tau_5^{24} = 0.06$ , where the basal plane is occupied by the three nitrogen atoms of **LH<sub>3</sub>** (N1, N2 and N3) and one oxygen atom of the monodentate tfa counter anion (O1), and the axial position is coordinated by an oxygen atom of another tfa counter anion (O2).

The structure of **Cu<sup>II</sup>(LH<sub>3</sub>)(tfa)<sub>2</sub>** was compared with those of the copper active sites of LPMOs (Fig. 3). The bond distances



Scheme 1. Synthesis of ligand **LH<sub>3</sub>** and **Cu<sup>II</sup>(LH<sub>3</sub>)(tfa)<sub>2</sub>**.

and angles around the copper centre matched well within  $\pm 0.1$  Å and  $\pm 3^\circ$ , respectively.<sup>7,8</sup> More importantly, the twist angle of the two imidazole rings in **Cu<sup>II</sup>(LH<sub>3</sub>)(tfa)<sub>2</sub>** was 75°, which is very close to the average value of the reported copper(II) sites in LPMOs, that is 72°. Therefore, the Histidine Brace structural

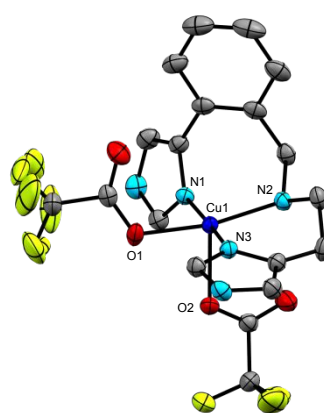


Fig. 2. An ORTEP drawing of the crystal structure of **Cu<sup>II</sup>(LH<sub>3</sub>)(tfa)<sub>2</sub>** with 50% ellipsoid probability. Hydrogen atoms are omitted for clarity. Rotational disorder was observed in trifluoromethyl group at the equatorial position.

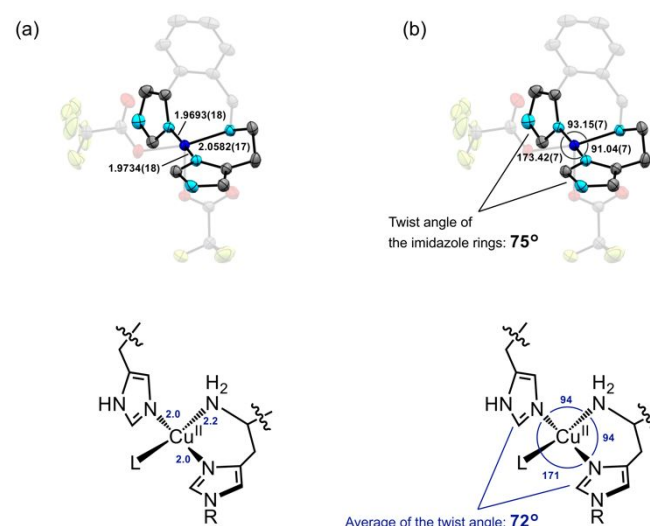


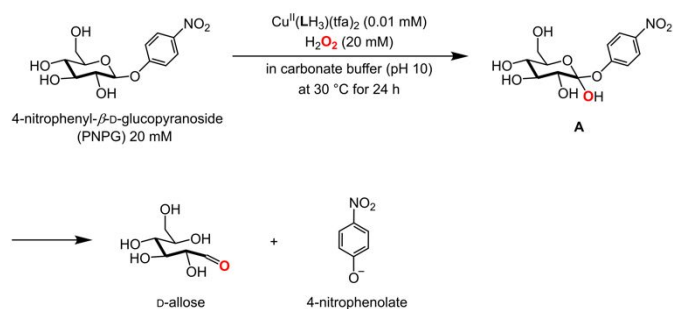
Fig. 3. (a) Comparison of the bond lengths [Å] and (b) the angles [deg] of **Cu<sup>II</sup>(LH<sub>3</sub>)(tfa)<sub>2</sub>** to those of the copper(II) sites in LPMOs (average values).

motif is well replicated by our simple model system. This is the first example of the structural model of the copper active sites bearing the Histidine Brace motif.

Physicochemical properties of our model complex were also compared to those of the enzymes. The UV-vis absorption (Fig. S3) band at 662 nm ( $\epsilon = 83 \text{ M}^{-1} \text{ cm}^{-1}$ ) was ascribed to a typical d–d band for the copper(II) complexes with a square pyramidal geometry. The  $\lambda_{\text{max}}$  and its  $\epsilon$  values are similar to those of LPMOs.<sup>8</sup> The electron paramagnetic resonance (EPR) spectrum of the complex was a typical one for a copper(II) complex with a tetragonal geometry having  $g_{\parallel}$  value as 2.266, and  $g_{\perp}$  value as 2.062 (Fig. S4), which are also very close to those of LPMOs.<sup>8</sup> A cyclic voltammetric measurement gave a quasi-reversible redox couple at 323 mV vs. SHE due to the Cu(II)/Cu(I) redox couple (Fig. S5), which is within the range of redox potentials of LPMOs so far been reported (155–370 mV).<sup>8</sup> It should be noted that the redox potentials of other model copper(II) complexes bearing imidazolyl groups at the *trans*-position but with small twist angles exhibited much lower redox potential less than 100 mV (Fig. S6, Table S2).<sup>18, 20, 25–30</sup> Overall, our model complex can also reproduce the physicochemical features of the active sites of LPMOs.

Catalytic activity of our model complex for oxidative cleavage of a glycosidic bond of 4-nitrophenyl  $\beta$ -D-glucopyranoside (PNPG), a model substrate of polysaccharide, was investigated using  $\text{H}_2\text{O}_2$  as an oxidant (Scheme 2).  $\text{H}_2\text{O}_2$  was also used in the shunt pass of the enzymatic reaction.<sup>31</sup> The reaction was monitored by following the formation of 4-nitrophenolate product ( $\lambda_{\text{max}} = 400 \text{ nm}$ ,  $\epsilon = 1.9 \times 10^4 \text{ M}^{-1} \text{ cm}^{-1}$ ). The spectral change during the first 1 h of the reaction is shown in Figs. S7(a) and (b), where the absorption band around 400 nm due to the product increased linearly, and after 24 h, total turnover number (TON) of the catalyst reached 58, where the yield of 4-nitrophenolate was 2.9% based on the substrate and oxidant (Fig. S7(c)).<sup>‡</sup> The product analyses were also performed using HPLC and GC-MS to confirm the formation of 4-nitrophenolate and D-allose, respectively (See, the Supplementary Information). D-allose is derived from the hydroxylated product of PNPG (A) as reported by Mayilmurugan, et al. in ref 19 (Scheme 2). These product analysis results confirmed that the oxidation reaction of PNPG proceeds. The kinetic analysis was carried out by following the absorption change at 400 nm due to the formation of 4-nitrophenolate (Figs. S9(a) and (b)). The observed reaction rate ( $V$  [ $\mu\text{M min}^{-1}$ ]) exhibited linear dependence both on the concentrations of the substrate (PNPG) and oxidant ( $\text{H}_2\text{O}_2$ ) as shown in Fig. 4.<sup>‡</sup> These results indicate that the turn over limiting step of the catalytic reaction is the substrate oxidation step by a reactive species generated by the reaction of the copper(II) complex and  $\text{H}_2\text{O}_2$  as depicted in Fig. S10(a).

As a model reaction of pMMO, the catalytic activity of the complex in the cyclohexane hydroxylation was also investigated using  $\text{H}_2\text{O}_2$  as an oxidant (Scheme 3).<sup>‡</sup> After 18 h, TON of the catalyst was 26, and cyclohexanol was obtained in a 5.2 percent yield based on the oxidant, and the product selectivity of cyclohexanol against cyclohexanone was 96%. The catalytic activity of this complex was comparable to those of other model complexes, but not so significantly high, probably due to the low miscibility of the complex and alkane substrate.



Scheme 2. Model reaction for LPMOs.

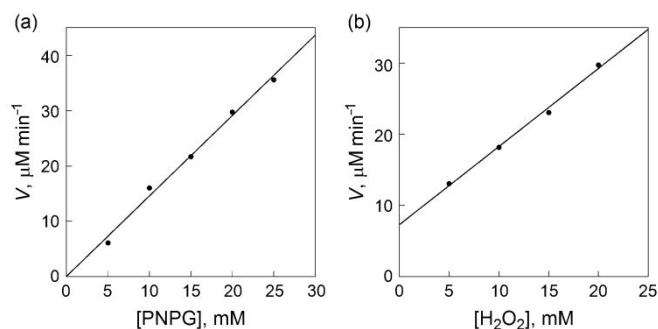
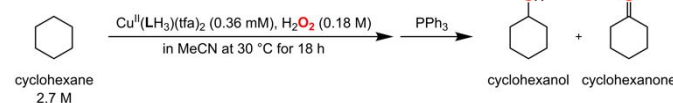


Fig. 4. Plots of  $V$  against the concentrations of (a) the substrate (PNPG) and (b) the oxidant ( $\text{H}_2\text{O}_2$ ). The reactions were carried out in the presence of  $[\text{Cu}^{\text{II}}(\text{LH}_3)(\text{tfa})_2]$  (0.2 mM) in carbonate buffer (pH 10) at 30 °C.



Scheme 3. Model reaction for pMMO.

In summary, a mononuclear copper(II) complex bearing a Histidine Brace motif was designed and successfully synthesised. The geometrical and physicochemical properties were similar to those of the active sites of LPMOs. Particularly, the electrochemical property of the complex is very similar to those of LPMOs, which may be attributed to a larger twist angle between the two imidazolyl rings at the *trans*-position. In addition, catalytic activity of the copper(II) complex was evaluated in the oxidative cleavage of the glycosidic bond of a polysaccharide model compound and the selective oxidation of inert alkane such as cyclohexane. Thus, the present complex can be regarded as the first example of a precise model complex showing both the structural characteristics and reactivity of the active sites of LPMOs and pMMO. The role of Histidine Brace has yet to be clarified. However, it is obvious that our complex bearing Histidine Brace structural motif shows the similar characteristics to those of the enzymatic systems, especially the relatively high redox potential of Cu(II)/Cu(I). The interactions between the d orbitals of the copper ion and the p orbitals of the imidazole groups might be important to dictate such interesting physicochemical properties. Further studies are being undertaken to evaluate the roles of Histidine Brace not only on the physicochemical properties but also the reactivity of the model complex.

This work was supported by CREST, JST (JPMJCR16P1) and by Grant-in-Aid for Challenging Research (Exploratory) (19K22201) from JSPS.

### Conflicts of interest

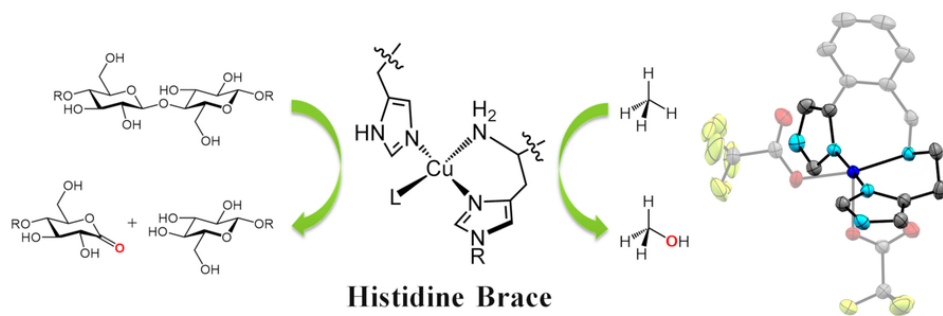
There are no conflicts to declare.

### Notes and references

<sup>‡</sup> A small amount of 4-nitrophenolate was detected in the absence of either H<sub>2</sub>O<sub>2</sub> or the complex, due to the hydrolysis of PNPg in a basic condition (Fig. S7(c)). The intercept on the y-axis of Fig. 4(b) corresponds to the reaction rate of self-hydrolysis of PNPg.

<sup>§</sup> The reaction mixture was treated with triphenylphosphine (PPh<sub>3</sub>) after the reaction. Hydroxylation of alkanes with H<sub>2</sub>O<sub>2</sub> often gives substantial amounts of corresponding alkyl hydroperoxide derivatives, and PPh<sub>3</sub> quantitatively converts the hydroperoxide compounds to corresponding alcohols.<sup>32</sup>

1. R. A. Sheldon, *Green Chemistry*, 2014, **16**, 950-963.
2. G. R. Hemsworth, E. M. Johnston, G. J. Davies and P. H. Walton, *Trends Biotechnol.*, 2015, **33**, 747-761.
3. T. J. Lawton and A. C. Rosenzweig, *J. Am. Chem. Soc.*, 2016, **138**, 9327-9340.
4. G. Vaaje-Kolstad, B. Westereng, S. J. Horn, Z. Liu, H. Zhai, M. Sorlie and V. G. Eijsink, *Science*, 2010, **330**, 219-222.
5. R. J. Quinlan, M. D. Sweeney, L. Lo Leggio, H. Otten, J. C. Poulsen, K. S. Johansen, K. B. Krogh, C. I. Jorgensen, M. Tovborg, A. Anthonsen, T. Tryfona, C. P. Walter, P. Dupree, F. Xu, G. J. Davies and P. H. Walton, *Proc. Natl. Acad. Sci. U.S.A.*, 2011, **108**, 15079-15084.
6. K. K. Meier, S. M. Jones, T. Kaper, H. Hansson, M. J. Koetsier, S. Karkehabadi, E. I. Solomon, M. Sandgren and B. Kelemen, *Chem. Rev.*, 2018, **118**, 2593-2635.
7. L. Ciano, G. J. Davies, W. B. Tolman and P. H. Walton, *Nat. Catal.*, 2018, **1**, 571-577.
8. V. V. Vu and S. T. Ngo, *Coord. Chem. Rev.*, 2018, **368**, 134-157.
9. R. L. Lieberman and A. C. Rosenzweig, *Nature*, 2005, **434**, 177-182.
10. R. Balasubramanian and A. C. Rosenzweig, *Acc. Chem. Res.*, 2007, **40**, 573-580.
11. M. O. Ross and A. C. Rosenzweig, *J. Biol. Inorg. Chem.*, 2017, **22**, 307-319.
12. R. Balasubramanian, S. M. Smith, S. Rawat, L. A. Yatsunyk, T. L. Stemmler and A. C. Rosenzweig, *Nature*, 2010, **465**, 115-119.
13. K. Yoshizawa, *Bull. Chem. Soc. Jpn.*, 2013, **86**, 1083-1116.
14. V. C. Wang, S. Maji, P. P. Chen, H. K. Lee, S. S. Yu and S. I. Chan, *Chem. Rev.*, 2017, **117**, 8574-8621.
15. L. Cao, O. Calderaru, A. C. Rosenzweig and U. Ryde, *Angew. Chem. Int. Ed.*, 2018, **57**, 162-166.
16. M. O. Ross, F. MacMillan, J. Wang, A. Nisthal, T. J. Lawton, B. D. Olafson, S. L. Mayo, A. C. Rosenzweig and B. M. Hoffman, *Science*, 2019, **364**, 566-570.
17. S. Y. Ro, L. F. Schachner, C. W. Koo, R. Purohit, J. P. Remis, G. E. Kenney, B. W. Liauw, P. M. Thomas, S. M. Patrie, N. L. Kelleher and A. C. Rosenzweig, *Nat. Commun.*, 2019, **10**, 2675.
18. A. L. Concia, M. R. Beccia, M. Orio, F. T. Ferre, M. Scarpellini, F. Biaso, B. Guigliarelli, M. Reglier and A. J. Simaan, *Inorg. Chem.*, 2017, **56**, 1023-1026.
19. S. Muthuramalingam, D. Maheshwaran, M. Velusamy and R. Mayilmurugan, *J. Catal.*, 2019, **372**, 352-361.
20. A. C. Neira, P. R. Martínez-Alanis, G. Aullón, M. Flores-Alamo, P. Zerón, A. Company, J. Chen, J. B. Kasper, W. R. Browne, E. Nordlander and I. Castillo, *ACS Omega*, 2019, **4**, 10729-10740.
21. D. E. Diaz, M. Bhadra and K. D. Karlin, *Inorg. Chem.*, 2019, **58**, 13746-13750.
22. S. Vichier-Guerre, L. Dugué and S. Pochet, *Tetrahedron Lett.*, 2014, **55**, 6347-6350.
23. Y. Shimasaki, H. Kiyota, M. Sato and S. Kuwahara, *Tetrahedron*, 2006, **62**, 9628-9634.
24. A. W. Addison, T. N. Rao, J. Reedijk, J. Vanrijn and G. C. Verschoor, *J. Chem. Soc., Dalton Trans.*, 1984, 1349-1356.
25. F. T. Ferre, J. A. L. C. Resende, J. Schultz, A. S. Mangrich, R. B. Faria, A. B. Rocha and M. Scarpellini, *Polyhedron*, 2017, **123**, 293-304.
26. M. Scarpellini, A. Neves, R. Horner, A. J. Bortoluzzi, B. Szpoganics, C. Zucco, R. A. N. Silva, V. Drago, A. S. Mangrich, W. A. Ortiz, W. A. C. Passos, M. C. B. de Oliveira and H. Terenzi, *Inorg. Chem.*, 2003, **42**, 8353-8365.
27. L. S. Long, Y. X. Tong, X. M. Chen and L. N. Ji, *J. Chem. Crystallogr.*, 1999, **29**, 409-412.
28. L. S. Long, Y. X. Tong, X. L. Yu, X. M. Chen, L. N. Ji and T. C. W. Mak, *Transition Met. Chem.*, 1999, **24**, 49-51.
29. I. Castillo, A. C. Neira, E. Nordlander and E. Zeglio, *Inorg. Chim. Acta*, 2014, **422**, 152-157.
30. C. Place, J. L. Zimmermann, E. Mulliez, G. Guillot, C. Bois and E. C. Chottard, *Inorg. Chem.*, 1998, **37**, 4030-4039.
31. A. Paradisi, E. M. Johnston, M. Tovborg, C. R. Nicoll, L. Ciano, A. Dowle, J. McMaster, Y. Hancock, G. J. Davies and P. H. Walton, *J. Am. Chem. Soc.*, 2019, **141**, 18585-18599.
32. G. B. Shul'pin, *J. Mol. Catal. A: Chem.*, 2002, **189**, 39-66.



The **first example** of structural and functional model of Histidine Brace

80x32mm (300 x 300 DPI)